Ligand and Tetrathiometalate Effects in Induced Internal Electron Transfer Reactions

C. A. McConnachie and E. I. Stiefel*

Corporate Research, Exxon Research and Engineering Co., Route 22 East, Annandale, New Jersey 08801

Received June 16, 1998

New rhenium sulfide complexes, $[Re^{IV}_2(\mu\text{-}S)_2(\mu\text{-}S_2)(\mu\text{-}S_2COR)(S_2COR)_2]^-$ and $[Re^{IV}_2(\mu\text{-}S)_2(S_2COR)_4]$, and a new tungsten sulfide complex, $[WS(S_2)(S_2CC_6H_5)_2]$, have been synthesized and isolated via induced internal redox reactions involving the appropriate tetrathiometalate and 1,1-dithiolate disulfide. The red complex $[Re^{IV}_2(\mu\text{-}S)_2(\mu\text{-}S_2)(\mu\text{-}S_2COR)(S_2COR)_2]^-$, **1**, was isolated from the reaction of dialkylxanthogen disulfide, $[(ROCS_2)_2]$, and tetraethylammonium tetrathioperrhenate, $[Et_4N][Re^{VII}S_4]$. Crystal structure analysis of **1** reveals an edge-sharing $(\mu\text{-}S)_2$ bioctahedron containing both bridging disulfide and xanthate ligands. This reaction is compared to the known reaction between tetraalkylthiuram disulfide, $[(R_2NCS_2)_2]$, and $[Et_4N][ReS_4]$, which produces the green complex $[Re^{IV}_2(\mu\text{-}S)_2(S_2CNR_2)_4]$. The corresponding green alkyl xanthate analogue, $[Re^{IV}_2(\mu\text{-}S)_2(S_2COR)_4]$, **2**, was synthesized by a simple redox reaction between rhenium pentachloride, $ReCl_5$, and potassium alkyl xanthate, $[K(S_2COR)]$. Comparing **1** with other known $[ReS_4]^-$/1,1-dithiolate disulfide reaction products, such as $[Re^{IV}_2(\mu\text{-}S)_2(S_2CNR_2)_4]$ and $[Re^{III}(S_2CC_6H_5)(S_3CC_6H_5)_2]$, shows a correlation between the electron-donating ability of the ligand and the nature of the reaction product. Reactions of $[Et_4N]_2[Mo^{VI}S_4]$, $[Et_4N][Re^{VII}S_4]$, or $[Et_4N]_2[W^{VI}S_4]$ with dithiobenzoate disulfide, $[(S_2CC_6H_5)_2]$, reveal a correlation between the ligand-to-metal charge transfer energy band ($LMCT_1$) of the tetrathiometalate and the reaction product. The known purple complex $[Mo^{IV}(S_2CC_6H_5)_4]$ and two new green complexes, $[Re^{III}(S_2CC_6H_5)(S_3CC_6H_5)_2]$ (recently communicated) and $[W^{VI}S(S_2)(S_2CC_6H_5)_2]$, were isolated from related reactions.

Introduction

Transition metal sulfide systems are prominent in both biological and industrial catalysts. Sulfur-coordinated transition metals engage in facile electron and proton transfer processes, which are important for active-site turnover in biological systems.[1] In industry, metal sulfides (such as MoS_2 and WS_2) are central to hydrotreating catalysis, including the removal of sulfur (hydrodesulfurization), nitrogen (hydrodenitrogenation), oxygen (hydrodeoxygenation), and metals (hydrodemetalation) from petroleum fractions.[1−3] Because of their importance in existing systems, and their potential use in future systems, a better understanding of metal sulfide complexes may prove valuable in the design of next-generation catalysts.

Tetrathiometalate anions with fully oxidized, d^0 metal centers and fully reduced sulfide ligands undergo internal redox upon reaction with external oxidants.[4] In these reactions, bound sulfide ions (S^{2-}) serve as the reductant, forming disulfide (S_2^{2-}) or sulfur while reducing the metal center. For example, in the reaction of tetraethylammonium tetrathioperrhenate, $[Et_4N][ReS_4]$, with tetraalkylthiuram disulfide, $[(R_2NCS_2)_2]$,[4a] Re^{VII} is reduced to Re^{IV}, with the electrons coming from the oxidation of the sulfides (S^{2-}) bound to the rhenium:

$$2[Re^{VII}S_4]^- + 3[R_2NCS_2]_2 \rightarrow [Re^{IV}_2(\mu\text{-}S)_2(S_2CNR_2)_4] + 6\text{“}S^0\text{”} + 2[R_2NCS_2]^- \quad (1)$$

Hence, adding an oxidant, such as thiuram disulfide, to a solution of $[Et_4N][ReS_4]$ causes the reduction of the metal center by coordinated S^{2-}, which serves as the reductant for both the metal and the disulfide. Such a process is termed an induced internal electron transfer.[4b,5]

Recently, we briefly reported the reaction of dithiobenzoate disulfide with $[Et_4N][ReS_4]$ to produce $[Re^{III}(S_2CC_6H_5)(S_3CC_6H_5)_2]$.[6] In this paper, we describe this chemistry in greater detail and seek to integrate it with other 1,1-dithiolate reactions. To broaden our understanding of ligand and tetrathiometalate effects on induced internal redox reactions, we compare the

(1) *Transition Metal Sulfur Chemistry: Biological and Industrial Significance;* Stiefel, E. I., Matsumoto, K., Eds.; ACS Symposium Series 653; American Chemical Society: Washington, DC, 1996.

(2) (a) Chianelli, R. R.; Daage, M.; Ledoux, M. *Adv. Catal.* **1994**, *40*, 177. (b) Rakowski DuBois, M. *Chem. Rev.* **1989**, *89*, 1. (c) H. Topsøe, H.; Clausen, B. S.; Massoth, F. E. *Hydrotreating Catalysis: Science and Technology*; Springer-Verlag: Berlin, 1996. (d) Prins, R.; DeBeer, V. H. J.; Somorjai, G. A. *Catal. Rev.—Sci. Eng.* **1989**, *31*, 1.

(3) (a) Weisser, O.; Landa, S. *Sulfide Catalysts, Their Properties and Applications*; Pergamon Press: New York, 1973. (b) Stiefel, E. I. In *Kirk-Othmer Encyclopedia of Chemical Technology,* 4th ed.; Kroschwitz, J. I., Exec. Ed.; Howe-Grant, M., Ed.; John Wiley & Sons: New York, 1995; Vol. 16, pp 940−962.

(4) (a) Murray, H. H.; Wei, L.; Sherman, S. E.; Greaney, M. A.; Eriksen, K. A.; Carstensen, B.; Halbert, T. R.; Stiefel, E. I. *Inorg. Chem.* **1995**, *34*, 841−853. (b) Harmer, M. A.; Halbert, T. R.; Pan, W.-H.; Coyle, C. L.; Cohen, S. A.; Stiefel, E. I. *Polyhedron* **1986**, *5*, 341−347. (c) Pan, W.-H.; Halbert, T. R.; Hutchings, L. L.; Stiefel, E. I. *J. Chem. Soc., Chem. Commun.* **1985**, 927−929. (d) Wei, L.; Halbert, T. R.; Murray, H. H., III; Stiefel, E. I. *J. Am. Chem. Soc.* **1990**, *112*, 6431−6433. (e) Draganjac, M.; Simhon, E.; Chan, L. T.; Kanatzidais, M.; Baenziger, N. C.; Coucouvanis, D. *J. Am. Chem. Soc.* **1982**, *21*, 3321−3332. (f) Simhon, E. D.; Baenziger, N. C.; Kanatzidis, M.; Draganjac, M.; Coucouvanis, D. *J. Am. Chem. Soc.* **1981**, *103*, 1218−1219. (g) Müller, A.; Sarkar, S.; Bhattacharyya, R. G.; Pohl, S.; Dartmann, M. *Angew. Chem., Int. Ed. Engl.* **1978**, *17*, 535. (h) Sarkar, S.; Ansari, M. A. *J. Chem. Soc., Chem. Commun.* **1986**, 324. (i) Ansari, M. A.; Chandrasekaran, J.; Sarkar, S. *Inorg. Chem.* **1988**, *27*, 763.

(5) Taube, H. *Electron Transfer Reactions of Complex Ions in Solution*; Academic Press: New York, 1970.

(6) McConnachie, C. A.; Stiefel, E. I. *Inorg. Chem.* **1997**, *36*, 6144−6145.

10.1021/ic980674z CCC: $18.00
Published on Web 02/17/1999

internal redox reactions of dialkylxanthogen disulfide, $[(ROCS_2)_2]$, dithiobenzoate disulfide, $[(C_6H_5CS_2)_2]$, and tetraalkylthiuram disulfide, $[(R_2NCS_2)_2]$, with $[Et_4N][ReS_4]$. Additionally, reactions of dithiobenzoate disulfide with tetrathiomolybdate, $[Et_4N]_2[Mo^{VI}S_4]$, and tetrathiotungstate, $[Et_4N]_2[W^{VI}S_4]$, are reported. A comparison of the chemistry for the dialkyl xanthate, dithiobenzoate, and dithiocarbamate ligands is given, as well as a comparison of the tetrathiomolybdate, tetrathiotungstate, and tetrathioperrhenate chemistry. The resultant trends highlight the important role of both ligand and tetrathiometalate in induced internal electron transfer processes.

Experimental Section

Materials and Syntheses. $[NH_4][ReO_4]$ was purchased from Engelhard Corp. and used as received. $[NH_4]_2[MoS_4]$ and $[NH_4]_2[WS_4]$ were purchased from SPEX. All other solvents (Sure-Seal) and reagents were purchased from Aldrich and used as obtained unless stated otherwise. The tetrabutylammonium hexafluorophosphate salt used for electrochemical experiments was recrystallized, dried, and stored in a glovebox. All syntheses were performed under an argon atmosphere using standard Schlenk-line techniques. All solid products were reasonably air-stable. $[Et_4N][ReS_4]$,[7] $[Et_4N]_2[MoS_4]$,[8] $[Et_4N]_2[WS_4]$,[9] dialkylxanthogen disulfide,[10,11a,12] and dithiobenzoate disulfide[4a,7] were synthesized according to literature procedures. Specific, yet representative, syntheses are given for the isobutyl derivative of the xanthogen disulfide. Similar procedures for isopropyl and *n*-butyl derivatives give similar results.

Synthesis of $[(CH_3CH_2)_4N][Re^{IV}_2(\mu\text{-}S)_2(\mu\text{-}S_2)(\mu\text{-}S_2COCH_2CH(CH_3)_2)(S_2COCH_2CH(CH_3)_2)_2]$, 1. A 1:1.5 mixture of $[Et_4N][ReS_4]$ (10 mmol, 4.4 g) and $[(CH_3)_2CHCH_2OCS_2)_2]$ (15 mmol, 4.5 g) was stirred for 3 days at room temperature in 50 mL of dry acetonitrile under an inert atmosphere. The resulting red mixture was filtered and the filtrate pumped off. Single crystals suitable for X-ray diffraction were obtained by slow diffusion of hexane into a saturated tetrahydrofuran solution, resulting in a 38% yield of pure material. This low yield is attributed to difficulty in removing impurities from the product. For example, during the course of the reaction, some of the product precipitated as a red powder. The addition of solvents such as CH_3CN/ether or THF/hexane led to the remainder of the product separating as an oil. Concentrating the solution and holding it at −20 °C also led to the formation of an oil. IR and UV−vis spectra showed that the oil contained a small amount of elemental sulfur as an impurity. Anal. Found (calcd): C, 24.93 (25.61); H, 4.60 (4.39); N, 2.55 (1.30); S, 29.75 (29.72). ^{1}H NMR (CD_3CN, 303 K): δ 4.95 (terminal ligands; CH_2, d, 4), 4.00 (bridging ligands; CH_2, d, 2), 3.16 (from cation; CH_2, q, 8), 2.60 (terminal ligands; CH, m, 2), 2.35 (bridging ligands; CH, m, 1), 0.84−1.30 (terminal and bridging ligands plus cation; CH_3, m). UV−vis/NIR (nm, acetonitrile solution): 920 (ϵ = 492 M^{-1} cm^{-1}), 475 (ϵ = 5528 M^{-1} cm^{-1}), 422 (ϵ = 7326 M^{-1} cm^{-1}), 310 (ϵ = 18 202 M^{-1} cm^{-1}). IR (cm^{-1}, KBr pressed pellet): 411 (m, Re−S), 516 (w, S−S), 787 (m), 899 (w), 937 (m, C−S), 964 (m, C−S), 999 (m, C−O), 1049 (s, C−O), 1173 (s), 1223 (s, C═S), 1396 (m), 1456 (s).

Synthesis of $[Re^{IV}_2(\mu\text{-}S)_2(S_2COCH_2CH_2CH_2CH_3)_4]$, 2. A 1:4 mixture of $ReCl_5$ (0.61 mmol, 0.22 g) and $K[S_2COCH_2CH_2CH_2CH_3]$ (2.7 mmol, 0.51 g) was stirred for 6 days at room temperature in 50 mL of dry acetonitrile under an inert atmosphere. The green mixture was filtered and the filtrate evaporated. The isolated solid was washed in acetonitrile and ether. The yield was 31.0%. Single crystals suitable for X-ray diffraction were obtained by layering a saturated methylene chloride solution with hexane. Anal. Found (calcd): C, 23.26 (23.24); H, 3.36 (3.51); S, 28.75 (31.02). ^{1}H NMR ($CDCl_3$, 303 K): δ 4.25 (CH_2, m, 2), 2.10 (CH, m, 1), 0.96 (CH_3, m, 3). UV−vis/NIR (nm, CH_2Cl_2 solution): 924 (ϵ = 591M^{-1} cm^{-1}), 729 (ϵ = 1383 M^{-1} cm^{-1}), 631 (ϵ = 3642 M^{-1} cm^{-1}), 380 (ϵ = 6491 M^{-1} cm^{-1}), and a shoulder at 295 (ϵ = 16 228 M^{-1} cm^{-1}). IR (cm^{-1}, KBr pressed pellet): 426 (m, Re−S), 893 (w), 933 (w, C−S), 964 (m, C−S), 1047 (s, C−O), 1178 (w), 1260 (s, C═S), 1377 (m), 1466 (m).

Synthesis of $[Re(S_2CC_6H_5)(S_3CC_6H_5)_2]$, 3. The synthesis and characterization of **3** has been reported previously.[6]

Synthesis of $[Mo^{IV}(S_2CC_6H_5)_4]$, 4. A 1:3 mixture of $[Et_4N]_2[MoS_4]$ (0.52 mmol, 0.25 g) and $[(C_6H_5CS_2)_2]$ (1.5 mmol, 0.47 g) was stirred overnight at room temperature in 50 mL of dry methylene chloride under an inert atmosphere. The mixture was filtered, and the filtrate was reduced. A dark purple powder was isolated by filtration and washed with acetonitrile and then ether. Purple single crystals suitable for X-ray diffraction were obtained by layering a solution of tetrahydrofuran with hexane. The yield of the crystalline material was 69%. X-ray diffraction analysis revealed the complex to be $[Mo^{IV}(S_2CC_6H_5)_4]$.[13] NMR, UV−vis/NIR, and IR spectra agree with reported values.[14]

Synthesis of $[Et_4N][W^{VI}O(S_2)_2(S_2CC_6H_5)]$, 5, and $[W^{VI}S(S_2)(S_2CC_6H_5)_2]$, 6. A 1:3 mixture of $[Et_4N]_2[WS_4]$ (0.51 mmol, 0.29 g) and $[(C_6H_5CS_2)_2]$ (1.5 mmol, 0.47 g) was stirred for 1 h at ambient temperature in 50 mL of dry methylene chloride under an inert atmosphere. The resulting green mixture was filtered in air, and the filtrate was collected and concentrated. The product was purified by column chromatography (silica gel, 60−200 mesh, using 1:1 hexane/$CHCl_3$ as eluent). Single crystals suitable for X-ray diffraction were obtained by layering a solution of tetrahydrofuran with hexane. The crystals isolated were red (from the green solution) and proved to be the oxygen-containing material $[Et_4N][WO(S_2)_2(S_2CC_6H_5)]$. Crystals of the green species (the major product) suitable for X-ray diffraction have not been isolated, but other methods of characterization (described under Results) show the complex to be $[W^{VI}S(S_2)(S_2CC_6H_5)_2]$. Characterization data for the red $[Et_4N][WO(S_2)_2(S_2CC_6H_5)]$ product are as follows. IR (cm^{-1}, KBr pressed pellet): 314 (w, W−S), 399 (w, W−S), 522 (m, S−S), 617 (w), 662 (w), 694 (w), 777 (m), 928 (s, W═O), 1015 (s, C−S), 1180 (w), 1242 (m), 1302 (w), 1398 (m), 1443 (s). UV−vis/NIR (nm, methylene chloride solution): 585 (ϵ = 283 M^{-1} cm^{-1}), 475 (ϵ = 1060 M^{-1} cm^{-1}), 388 (ϵ = 2835 M^{-1} cm^{-1}), 318 (ϵ = 11 765 M^{-1} cm^{-1}). Characterization data for the green $[W^{VI}S(S_2)(S_2CC_6H_5)_2]$ microcrystals (obtained from a solution of $CHCl_3$ layered with hexane) are as follows. IR (cm^{-1}, KBr pressed pellet): 318 (w, W−S), 399 (w, W−S), 451 (w, W−S), 498 (m, W═S),[8,9] 540 (w, S−S),[4c,15] 664−677 (d, s), 762 (s), 939 (C−S, m), 995 (C−S, s), 1177 (m), 1267 (s), 1445 (m), 1584 (m). UV−vis/NIR (nm, methylene chloride solution): 809 (shoulder, ϵ = 400 M^{-1} cm^{-1}), 622 (ϵ = 1398 M^{-1} cm^{-1}), 429 (shoulder, ϵ = 4597 M^{-1} cm^{-1}), 330 (ϵ = 22 964 M^{-1} cm^{-1}). ^{1}H NMR (CD_2Cl_2, 303 K): δ 7.45 (m, 2), 7.60 (m, 2), 7.70 (m, 1), 7.80 (m, 1), 8.04 (d, 2), 8.20 (d, 2). ^{13}C NMR (THF-d_8, 299.1 K): δ 124.14 (C_{ph}), 125.20 (C_{ph}), 128.42 (C_{ph}), 129.98 (C_{ph}), 135.80 (C_{ph}), 138.62 (C_{ph}), 143.53 (C_{ph}), 146.76 (C_{ph}), 246.72 (CS_2), 247.43 (CS_2). Mass spectrum, *m*/*z* (highest peak in multiplet): 586. Anal. Found: C, 31.04; H, 2.02; S, 35.06. The yield of the microcrystalline material was 73%.

Physical Measurements. ^{1}H and ^{13}C NMR were obtained on a Varian 400 MHz spectrometer using tetramethylsilane as a reference (δ = 0 ppm). Infrared spectra were recorded on a Galaxy Series FTIR-5000 instrument from Mattson. Infrared spectra of samples were measured as KBr pressed pellets. UV−vis spectra were recorded on a Cary 5E UV−vis/NIR spectrophotometer. Mass spectra were recorded

(7) Wei, L.; Halbert, T. R.; Stiefel, E. I. U.S. Patent 4,997,962, 1991.
(8) Pan, W.-H.; Stiefel, E. I. U.S. Patent 4,588,829, **1986**.
(9) Stiefel, E. I.; Pan, W.-H.; Halbert, T. R. U.S. Patent 4,585,882, 1986.
(10) Ricard, L.; Karagiannidis, P.; Weiss, R. *Inorg. Chem.* **1973**, *12*, 2179−2182.
(11) (a) Hamilton, I. C.; Woods, R. *Aust. J. Chem.* **1979**, *32*, 2171−2179. (b) Winter, G.; Woods, R. *Sep. Sci.* **1973**, *8*, 261−267. (c) Winter, G. *Inorg. Nucl. Chem. Lett.* **1975**, *11*, 113−118. (d) Bond, A. M.; Sztajer, Z.; Winter, G. *Anal. Chim. Acta* **1976**, *84*, 37−46.
(12) Vella, P.; Zubieta, J. *J. Inorg. Nucl. Chem.* **1978**, *40*, 477−487.
(13) Bonamico, M.; Dessy, G.; Fares, V.; Scaramuzza, L. *J. Chem. Soc., Dalton Trans.* **1975**, 2079−2082.
(14) (a) Hyde, J.; Zubieta, J. *J. Inorg. Nucl. Chem.* **1977**, *39*, 289−296. (b) Roberie, T.; Hoberman, A. E.; Selbin, J. *J. Coord. Chem.* **1979**, *9*, 79−87. (c) Piovesana, O.; Sestili, L. *Inorg. Chem.* **1974**, *13*, 2745−2750. (d) Holste, V. G. Z. *Anorg. Allg. Chem.* **1976**, *425*, 57−66. (e) Roberie, T.; Bhacca, N. S.; Lankin, D.; Selbin, J. *Can. J. Chem.* **1980**, *58*, 2314−2317.
(15) Cohen, S. A.; Stiefel, E. I. *Inorg. Chem.* **1985**, *24*, 4657−4662.

Table 1. Crystallographic Data for **1**, **2**, **3**, and **5**

	1	**2**	**3**	**5**
formula	$C_{23}H_{47}NO_3Re_2S_{10}$	$C_{20}H_{36}O_4Re_2S_{10}$	$C_{21}H_{15}ReS_8$	$C_{15}H_{25}NOS_6W$
fw	1078.62	1033.49	710.01	611.57
space group	$P2_1$	$C2/m$	$P2_1/c$	$P2_1/n$
a (Å)	7.935(2)	8.602(2)	20.041(4)	14.018(3)
b (Å)	20.769(4)	25.089(5)	10.580(2)	11.407(2)
c (Å)	11.489(2)	8.366(2)	12.022(2)	14.591(3)
β (deg)	94.36(3)	104.06(3)	105.54(3)	110.71(3)
V (Å^3)	1887.9(7)	1751.4(6)	2455.9(8)	2182.4(8)
D_{calc} (g/cm^3)	1.897	1.960	1.920	1.861
Z	2	2	4	4
$\mu_{Mo\ K\alpha}$ (cm^{-1})	69.8	75	56	59
transm factors	0.271−0.836	0.081−0.140	0.496−0.973	0.413−0.519
θ range (deg)	2.03−25.96	2.51−26.47	2.19−27.47	2.33−24.97
no. of tot. reflns	4517	3873	5388	4002
no. of obsd reflns ($I > 2\sigma(I)$)	3713	1532	3958	2405
R^a	0.0407	0.0336	0.0441	0.060
$R_w{}^b$	0.1879	0.0783	0.1246	0.112

[a] $R = \sum||F_o| - |F_c||/\sum|F_o|$. [b] $R_w = \{\sum w(|F_o| - |F_c|)^2/\sum w|F_o|^2\}^{1/2}$.

on a Vacuum Generators VG ZAB2-SEQ mass spectrometer. Elemental analyses were performed by Quantitative Technologies, Inc., Whitehouse, NJ.

Electrochemistry. Electrochemical experiments were performed under argon at room temperature. Potentials were recorded relative to a nonaqueous $Ag/AgNO_3$ reference electrode. A solution of 0.1 M $[(CH_3CH_2CH_2CH_2)_4N][PF_6]$ in Aldrich Sure-Seal acetonitrile (**1**) or methylene chloride (**2** and **3**) was used as an electrolyte medium. Cyclic voltammetry was carried out using a BAS 100W electrochemical analyzer and an IBM voltammetric cell containing a platinum working electrode (area 75 mm^2) and a platinum wire auxiliary electrode. Corrections were made for *iR* drop.

Crystallographic Studies. A crystal of **1**, **2**, **3**, or **5** was mounted on an Enraf-Nonius CAD4-diffractometer (the X-ray diffraction analysis of **4** will not be discussed, since this structure was reported previously).[13] Unit cell parameters were determined from a least-squares refinement of 25 automatically centered reflections. Diffraction data were collected at 20 ± 2 °C. Six standard reflections monitored at intervals of every 3 h showed no significant change during the course of data collection. Crystal data and details of the data collection for all the compounds are given in Table 1. In the solution and refinement of these structures, the SHELXTL 5.0 software package was used.[16] The initial solutions were obtained by heavy-atom methods, data were corrected for absorption with empirical methods, and the structures were refined on F_o^2 with full-matrix least-squares analysis. Hydrogen atoms were placed at calculated positions and refined according to a riding model.

(a) $[(CH_3CH_2)_4N][Re^{IV}_2(\mu\text{-}S)_2(\mu\text{-}S_2)(\mu\text{-}S_2COCH_2CH(CH_3)_2)(S_2CO\text{-}CH_2CH(CH_3)_2)_2]$, 1. The $[NEt_4]^+$ cation is disordered, with α-C atoms occupying two different positions, which refined to occupancies of 0.54 and 0.46, around the N atom. All non-hydrogen atoms in the anion were refined anisotropically; the cation heavy atoms were refined isotropically. The final cycle of least-squares refinement on F_o^2 for 4136 data and 324 parameters converged to a value of $R_w(F_o^2) = 0.188$ for all data and to a value of $R = 0.041$ for those 3713 data having $F_o^2 \geq 2\sigma(F_o^2)$.

(b) $[Re^{IV}_2(\mu\text{-}S)_2(S_2COCH_2CH_2CH_2CH_3)_4]$, 2. The structure determination was complicated by poor crystal quality, complex site symmetry of the molecule, and libration down the alkyl chain of the xanthate ligands. The molecule is centered on a 0, 0, $^1/_2$ position and has 2/*m* site symmetry. Due to the 2/*m* symmetry, there are two independent xanthate ligands which provide all four ligands (two ligands per rhenium atom). The positions of these xanthate ligands were determined by comparing the compound to the analogous $Re_2(\mu\text{-}S)_2(S_2CNR_2)_4$ complex (the similarity of these two compounds was determined by comparing UV−vis and IR spectra).[4a]

(16) Sheldrick, G. M. *SHELXTL 5.0: An Integrated System for Solving, Refining, and Displaying Crystal Structures from Diffraction Data*; Siemens Analytical X-ray Instruments, Inc.: Madison, WI, 1994.

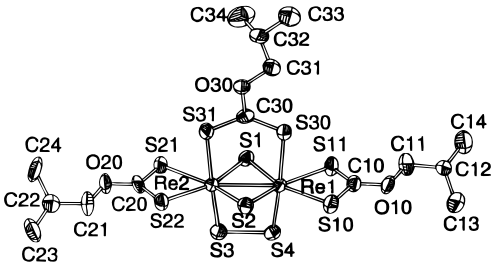

Figure 1. Molecular structure of $[(CH_3CH_2)_4N][Re_2(\mu\text{-}S)_2(\mu\text{-}S_2)(\mu\text{-}S_2\text{-}COCH_2CH\text{-}(CH_3)_2)(S_2COCH_2CH(CH_3)_2)_2]$.

Due to the disorder in the xanthate ligands, all atoms, except S_{30}, have occupancies of 0.5. However C_{11} and C_{21}, despite being in different alkyl groups, share the same position, and thus the combined occupancy of C_{11} and C_{21} is 1.0. Owing to the disorder in the structure and increasing libration of the C atoms down the alkyl chain (which results in increasing temperature factors), the C atom positions in the alkyl chains after C_{11}/C_{21} and their corresponding metrical details must be treated with caution (e.g., the standard deviations are probably much too small). The distances around the Re−S core and the xanthate ligands out to C_{11}/C_{21} appear reasonable.

The atoms in the alkyl chains C_{12}, C_{13}, C_{14}, C_{22}, C_{23}, and C_{24} were refined isotropically; the remaining atoms were refined anisotropically. The final cycle of least-squares refinement on F_o^2 for 1862 data and 109 parameters converged to a value of $R_w(F_o^2) = 0.078$ for all data and to a value of $R = 0.034$ for those 1532 data having $F_o^2 \geq 2\sigma(F_o^2)$.

(c) $[Re(S_2CC_6H_5)(S_3CC_6H_5)_2]$, 3. The final cycle of least-squares refinement on F_o^2 for 5216 data and 271 parameters converged to a value of $R_w(F_o^2) = 0.125$ for all data and to a value of $R = 0.044$ for those 3958 data having $F_o^2 \geq 2\sigma(F_o^2)$.

(d) $[(CH_3CH_2)_4N][W(O)(S_2)_2(S_2CC_6H_5)]$, 5. All non-hydrogen atoms were refined anisotropically. The final cycle of least-squares refinement on F_o^2 for 3835 data and 217 parameters converged to a value of $R_w(F_o^2) = 0.112$ for all data and to a value of $R = 0.060$ for those 2405 data having $F_o^2 \geq 2\sigma(F_o^2)$.

Results

Structural Descriptions. (a) $[(CH_3CH_2)_4N][Re^{IV}_2(\mu\text{-}S)_2(\mu\text{-}S_2)(\mu\text{-}S_2COCH_2CH(CH_3)_2)(S_2COCH_2CH(CH_3)_2)_2]$, 1. Selected interatomic distances and angles for **1** are given in Table 2. X-ray diffraction analysis established the edge-sharing bioctahedral dirhenium complex shown in Figure 1. The complex contains a bridging disulfide and a bridging isobutyl xanthate ligand. The coordination around each rhenium is distorted octahedral, with the distortion largely attributable to

Table 2. Selected Bond Lengths (Å) and Angles (deg) for $[(CH_3CH_2)_4N][Re^{IV}_2(\mu\text{-}S)_2(\mu\text{-}S_2)(\mu\text{-}S_2COCH_2CH(CH_3)_2)\text{-}(S_2COCH_2CH(CH_3)_2)_2]$, **1**

Bond Lengths			
Re(1)−Re(2)	2.6647(11)	S(3)−S(4)	2.117(7)
Re(1)−S(1)	2.302(5)	Re(1)−S(2)	2.300(5)
Re(1)−S(4)	2.259(5)	Re(1)−S(30)	2.518(5)
Re(2)−S(3)	2.262(5)	Re(2)−S(31)	2.462(5)
Re(2)−S(21)	2.480(4)	Re(2)−S(22)	2.465(4)
S(10)−C(10)	1.70(2)	S(11)−C(10)	1.65(2)
S(30)−C(30)	1.67(2)	S(31)−C(30)	1.68(2)
O(10)−C(10)	1.35(2)	O(10)−C(11)	1.46(2)
O(30)−C(30)	1.38(2)	O(30)−C(31)	1.46(2)

Bond Angles			
S(4)−Re(1)−S(2)	89.8(2)	S(2)−Re(1)−S(1)	108.8(2)
S(4)−Re(1)−S(11)	97.6(2)	S(2)−Re(1)−S(11)	159.4(2)
S(1)−Re(1)−S(11)	90.5(2)	S(11)−Re(1)−S(10)	70.1(2)
S(4)−Re(1)−S(30)	176.5(2)	S(1)−Re(1)−S(30)	89.9(2)
S(10)−Re(1)−S(30)	86.1(2)	S(3)−Re(2)−S(2)	90.4(2)
S(2)−Re(2)−S(1)	108.7(2)	S(3)−Re(2)−S(31)	177.3(2)
S(2)−Re(2)−S(31)	89.7(2)	S(3)−Re(2)−S(22)	96.7(2)
S(2)−Re(2)−S(22)	89.4(2)	S(1)−Re(2)−S(22)	161.1(2)
S(31)−Re(2)−S(22)	86.0(2)	S(22)−Re(2)−S(21)	70.3(2)
S(3)−Re(2)−Re(1)	83.05(12)	S(1)−Re(2)−Re(1)	54.56(12)
S(31)−Re(2)−Re(1)	94.81(11)	S(22)−Re(2)−Re(1)	143.96(12)
Re(2)−S(2)−Re(1)	70.87(14)	S(4)−S(3)−Re(2)	96.9(2)
S(2)−Re(1)−Re(2)	54.51(12)	S(11)−Re(1)−Re(2)	145.29(12)
S(30)−Re(1)−Re(2)	93.80(10)	Re(1)−S(1)−Re(2)	70.62(14)

the small bite of the $[S_2COCH_2CH(CH_3)_2]^-$ ligand.[17] The S−C bond lengths in the terminal and bridging ligands of **1** fall between a single S−C (1.729 Å) and a double S═C (1.620 Å) bond length in diethylxanthogen disulfide.[18] The C−O bond lengths in **1** fall between those of a single and a double bond, with the bridging xanthate ligand ($O_{30}-C_{30}$, 1.38(2) Å) having the longest C−O bond.[19] The Re−S bonds of the xanthate ligands, the Re−(μ-S) bonds, and the Re−S bonds to the disulfide are unexceptional. The Re−S bonds to the disulfide are the shortest, with 2.259(5) Å for Re_1-S_4 and 2.262(5) Å for Re_2-S_3. The disulfide bond length (S_3-S_4, 2.117(7) Å) is within the normal range for disulfides.[20] The Re_1-Re_2 bond length (2.665(1) Å) is longer than the Re−Re distance (2.546(1) Å) in the neutral dithiocarbamate complex $[Re_2(\mu\text{-}S)_2(S_2CN(CH_2CH(CH_3)_2)_2)_4]$.[4a]

(b) $[Re^{IV}_2(\mu\text{-}S)_2(S_2COCH_2CH_2CH_2CH_3)_4]$, 2. Selected interatomic distances and angles are given in Table 3. X-ray diffraction analysis established the edge-sharing bioctahedral dirhenium complex shown in Figure 2. This complex is very similar (i.e., in geometry and in Re−S and Re−Re bond lengths) to the reported dithiocarbamate complex $[Re_2(\mu\text{-}S)_2(S_2CN(CH_2CH(CH_3)_2)_2)_4]$.[4a] Each Re center is coordinated to six sulfur atoms in a distorted octahedral geometry, where the distortion is attributed to the small bite of the chelating ligands. The S−C bond lengths are shorter [1.59(2) Å ($S_{30C}-C_{10C}$) to 1.66(2) Å ($S_{10}-C_{10}$)], presumably due to greater double-bond character, than those in **1** [1.65(2)−1.72(2) Å]. The Re_1-Re_{1A} bond length (2.529(1) Å) is comparable to the Re−Re bond (2.546(1) Å) of $[Re_2(\mu\text{-}S)_2(S_2CN(CH_2CH(CH_3)_2)_2)_4]$.[4a] All other bond lengths and angles are unremarkable.

Table 3. Selected Bond Lengths (Å) and Angles (deg) for $[Re^{IV}_2(\mu\text{-}S)_2(S_2COCH_2CH_2CH_2CH_3)_4]$, **2**[a]

Bond Lengths			
Re(1)−Re(1)#1	2.5296(12)	Re(1)−S(1)	2.269(3)
Re(1)−S(30)	2.428(3)	Re(1)−S(20)	2.498(4)
Re(1)−S(10)	2.511(4)	S(20)−C(20)	1.66(2)
S(10)−C(10)	1.66(2)	S(30)#1−C(20)	1.63(2)
S(30)−C(10)	1.59(2)	O(10)−C(11)	1.68(2)
C(10)−O(10)	1.32(2)	C(11)−C(12)	1.36(3)
C(20)−O(20)	1.31(2)	O(20)−C(21)	1.66(2)

Bond Angles			
S(1)−Re(1)−S(1)#1	112.23(7)	S(1)−Re(1)−S(30)	96.99(6)
S(1)#1−Re(1)−S(30)	97.11(6)	S(1)−Re(1)−S(20)	84.36(12)
S(30)#2−Re(1)−S(30)	154.56(12)	S(30)#2−Re(1)−S(20)	90.44(12)
S(1)#1−Re(1)−S(20)	160.60(11)	S(30)−Re(1)−S(20)	69.95(11)
S(1)−Re(1)−S(10)	159.56(12)	S(1)#1−Re(1)−S(10)	84.41(12)
S(30)−Re(1)−S(10)	92.38(12)	S(30)#2−Re(1)−S(10)	68.19(11)
S(20)−Re(1)−S(10)	81.86(14)	S(1)−Re(1)−Re(1)#1	56.10(7)
Re(1)−S(1)−Re(1)#1	67.77(7)	C(10)−S(10)−Re(1)	85.3(6)
S(20)−Re(1)−Re(1)#1	139.25(10)	S(30)−Re(1)−Re(1)#1	102.72(6)
S(10)−Re(1)−Re(1)#1	138.86(10)	C(20)−S(20)−Re(1)	84.0(6)
O(10)−C(10)−S(10)	123.8(13)	S(30)−C(20)−S(20)	118.6(10)
C(10)−O(10)−C(11)	119.1(13)	C(12)−C(11)−O(10)	105(2)
O(20)−C(20)−S(30)	115.6(13)	O(20)−C(20)−S(20)	125.8(14)

[a] Symmetry transformations used to generate equivalent atoms: (#1) $-x, -y, -z+1$; (#2) $x, -y, z$; (#3) $-x+1, y, -z+2$.

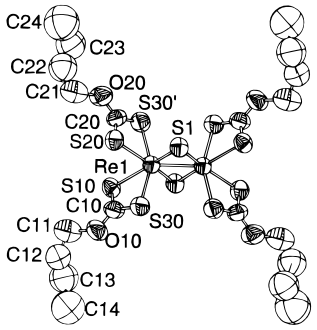

Figure 2. Molecular structure of $[Re_2(\mu\text{-}S)_2(S_2COCH_2CH_2CH_2CH_3)_4]$.

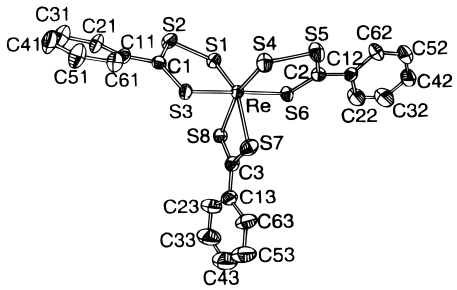

Figure 3. Molecular structure of $[Re(S_2CC_6H_5)(S_3CC_6H_5)_2]$.

(c) $[Re(S_2CC_6H_5)(S_3CC_6H_5)_2]$, 3. X-ray diffraction analysis established the six-coordinate, distorted octahedral structure shown in Figure 3. Structural results, including interatomic distances and angles, have been reported previously.[6]

(d) $[Et_4N][W^{VI}O(S_2)_2(S_2CC_6H_5)]$, 5. Selected interatomic distances and angles are given in Table 4. X-ray diffraction analysis established the seven-coordinate structure shown in Figure 4. The coordination around the W^{VI} metal center is distorted pentagonal bipyramidal, similar to that of other seven-coordinate mononuclear tungsten and molybdenum sulfide complexes.[21−26] Bond lengths and angles are similar to those in the known complexes $[Et_4N][Re(S_2CC_6H_5)_3CN]$,[10] $[WO(S_2)(S_2CN(CH_2CH_3))_2]$,[21] and $[WS(S_2)(S_2CNR_2)_2]$.[4c]

(17) (a) Kepert, D. L. *Prog. Inorg. Chem.* **1977**, *23*, 1−65. (b) Stiefel, E. I.; Brown, G. F. *Inorg. Chem.* **1972**, *11*, 434−436.
(18) Watanabe, Y. *Acta Crystallogr.* **1971**, *B27*, 644−649.
(19) (a) Merlino, S. *Acta Crystallogr.* **1969**, *B25*, 2270−2276. (b) Hyde, J.; Zubieta, J. *J. Inorg. Nucl. Chem.* **1977**, *39*, 289−296. (c) Nakamoto, K.; Fujita, J.; Condrate, R. A.; Morimoto, Y. *J. Chem. Phys.* **1963**, *39*, 423−427. (d) Chatt, J.; Duncanson, L. A.; Venanzi, L. M. *Nature* **1956**, *177*, 1042−1043. (e) Lewis, D. F.; Lippard, S. J.; Zubieta, J. A. *J. Am. Chem. Soc.* **1972**, *94*, 1563−1575.
(20) Carrillo, D. *Coord. Chem. Rev.* **1992**, *119*, 137−169.
(21) Broomhead, J. A.; Enemark, J. H.; Hammer, B.; Ortega, R. B.; Pienkowski, W. *Aust. J. Chem.* **1987**, *40*, 381−385.

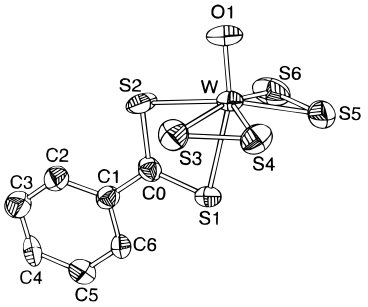

Figure 4. Molecular structure of $[WO(S_2)_2(S_2CC_6H_5)]$.

Table 4. Selected Bond Lengths (Å) and Angles (deg) for $[(CH_3CH_2)_4N][W^{VI}O(S_2)_2(S_2CC_6H_5)]$, **5**

Bond Lengths			
W(1)−O(1)	1.693(8)	W(1)−S(5)	2.363(4)
W(1)−S(4)	2.364(4)	W(1)−S(3)	2.402(4)
W(1)−S(6)	2.424(4)	W(1)−S(2)	2.517(4)
W(1)−S(1)	2.700(3)	S(1)−C(0)	1.670(12)
S(2)−C(0)	1.697(12)	S(3)−S(4)	2.053(5)
S(5)−S(6)	2.071(6)	C(0)−C(1)	1.46(2)
Bond Angles			
O(1)−W(1)−S(5)	105.9(3)	O(1)−W(1)−S(4)	103.5(3)
S(5)−W(1)−S(4)	85.22(14)	O(1)−W(1)−S(3)	98.7(3)
S(5)−W(1)−S(3)	133.93(14)	S(4)−W(1)−S(3)	51.02(13)
O(1)−W(1)−S(6)	97.2(3)	S(5)−W(1)−S(6)	51.2(2)
S(4)−W(1)−S(6)	135.6(2)	S(3)−W(1)−S(6)	159.88(13)
O(1)−W(1)−S(2)	93.5(3)	S(5)−W(1)−S(2)	133.10(14)
S(4)−W(1)−S(2)	131.61(14)	S(3)−W(1)−S(2)	82.06(13)
S(6)−W(1)−S(2)	84.8(2)	O(1)−W(1)−S(1)	159.5(3)
S(5)−W(1)−S(1)	87.65(12)	S(4)−W(1)−S(1)	92.72(13)
S(3)−W(1)−S(1)	81.70(12)	S(6)−W(1)−S(1)	79.09(12)
S(2)−W(1)−S(1)	66.13(10)	C(0)−S(1)−W(1)	86.2(4)
C(0)−S(2)−W(1)	91.8(4)	S(4)−S(3)−W(1)	63.5(2)
S(3)−S(4)−W(1)	65.45(14)	S(6)−S(5)−W(1)	65.9(2)
S(5)−S(6)−W(1)	62.9(2)	C(1)−C(0)−S(1)	124.3(9)
C(1)−C(0)−S(2)	120.1(9)	S(1)−C(0)−S(2)	115.7(7)

(e) $[W^{VI}S(S_2)(S_2CC_6H_5)_2]$, 6. Growing suitable crystals of the green species (the major product in the reaction between $[W^{VI}S_4]^{2-}$ and $[S_2CC_6H_5]_2$) for X-ray diffraction analysis was not successful. Nevertheless, a reasonable assignment of its chemical formula and structure can be made. IR, UV−vis, NMR, and mass spectra suggest that the green complex is likely $[W^{VI}S(S_2)(S_2CC_6H_5)_2]$. The IR spectrum displays a weak ν(S−S) stretch at 540 cm^{-1} and a ν(W═S) stretch at 498 cm^{-1},[4c,8,9,15] which are similar to the S−S (ν = 550 cm^{-1}) and W═S (ν = 500 cm^{-1}) stretches reported for the known dithiocarbamate complex $[WS(S_2)(S_2CNR_2)_2]$.[4c] ^{1}H NMR shows two chemically different ligands, with phenyl proton peaks at 7.45 (m, 2), 7.60 (m, 2), 7.70 (m, 1), 7.80 (m, 1), 8.04 (d, 2), and 8.20 (d, 2) ppm (a total of 10 protons for two phenyl rings). ^{13}C NMR shows eight distinct carbon peaks in the aromatic ring region (124.14, 125.20, 128.42, 129.98, 135.80, 138.62, 143.53, 146.76 ppm) and two carbon peaks in the thiocarbon (CS_2) region (246.72, 247.43 ppm). The NMR spectra indicate that the complex is likely diamagnetic, in agreement with a W^{VI} oxidation state or dinuclear formulation.

Unfortunately, analytical results do not unequivocally support the $[WS(S_2)(S_2CC_6H_5)_2]$ formulation. Found (versus calculated) values for $[WS(S_2)(S_2CC_6H_5)_2]$ (%): C, 31.04 (28.67); H, 2.02 (1.72); S, 35.06 (38.27). The dinuclear compound $[W^{IV}_2(\mu\text{-}S)_2(S_2CC_6H_5)_4]$ could fit the NMR and analytical data almost as well, with the following found (versus calculated) values (%): C, 31.04 (32.19); H, 2.02 (1.93); S, 35.06 (30.69). However, the IR spectrum of the green species (when compared to the IR spectrum of the analogous green complex, $[WS(S_2)(S_2CNR_2)_2]$)[4c] indicates the presence of a W═S stretch as well as a S−S stretch. In addition, the field desorption mass spectrum of the green species exhibits a strong peak at *m*/*z* 586, which corresponds to the mononuclear compound.

Finally, the isolation of the oxotungsten monomer $[WO(S_2)_2(S_2CC_6H_5)]$ from the reaction solution is an indicator that the green species is most likely mononuclear, undergoing hydrolysis along with decomposition or rearrangement, to form $[WO(S_2)_2(S_2CC_6H_5)]$. There is precedent for sulfidotungsten compounds being water sensitive. The preparation of $[NEt_4][W_2S_{12}]$ (made by reacting $[NH_4]_2[WS_4]$, sulfur, and $[Et_4N]Br$ in DMF at 110 °C)[15] was found to be quite water sensitive. Samples hydrolyzed during the synthesis and workup (as evidenced by the W═O stretch at 949 cm^{-1}), although once they were isolated as pure samples, no measurable decomposition or hydrolysis occurred after weeks in air at ambient temperatures.[15] Similarly, the green dithiobenzoate species, once removed from solution, was found to be stable in air.

Electrochemistry. The cyclic voltammogram of $[(CH_3CH_2)_4N][Re_2(\mu\text{-}S)_2(\mu\text{-}S_2)(\mu\text{-}S_2COCH(CH_3)_2)(S_2COCH(CH_3)_2)_2]$ in CH_3CN (vs $Ag/AgNO_3$) displays a reversible, one-electron oxidation at $E_{1/2} = -0.18$ V, indicating oxidation of the anionic $[Re_2(\mu\text{-}S)_2(\mu\text{-}S_2)(S_2COCH(CH_3)_2)_3]^-$ complex (Re^{IV}, Re^{IV}) to the neutral (Re^{V}, Re^{IV}) complex (Figure 5a). A quasi-reversible reduction occurs at $E_{1/2} = -1.55$ V implicating the dianionic $[Re_2(\mu\text{-}S)_2(\mu\text{-}S_2)(S_2COCH(CH_3)_2)_3]^{2-}$ complex (Re^{III}, Re^{IV}). On the first cathodic scan, a reduction peak at −0.77 V is observed, but on subsequent scans, this peak disappears. In older samples, which have undergone some decomposition, the reduction at −0.77 V does not disappear upon further cycling, and the reversible oxidation at −0.18 V becomes irreversible. The quasi-reversible reduction at −1.55 V, on the other hand, becomes more reversible (Figure 5b). Though the reasons for these changes in the cyclic voltammogram are not understood, there is precedent for this type of behavior. Similar changes have been observed in the cyclic voltammograms of $[Re_2(\mu\text{-}S)_2(S_2CNR_2)_4]$ complexes that are known to contain sulfur as an impurity.[4a]

The cyclic voltammogram of $[Re_2(\mu\text{-}S)_2(S_2COCH_2CH(CH_3)_2)_4]$ in CH_2Cl_2 (vs $Ag/AgNO_3$) contains one reversible one-electron reduction at $E_{1/2} = -1.00$ V, which is attributed to formation of the anion $[Re_2(\mu\text{-}S)_2(S_2COCH_2CH(CH_3)_2)_4]^-$ (Re^{III}, Re^{IV}; Figure 6a); one reversible oxidation at $E_{1/2} = 0.35$ V, forming the cationic (Re^{V}, Re^{IV}) complex $[Re_2(\mu\text{-}S)_2(S_2COCH_2CH(CH_3)_2)_4]^+$; and one quasi-reversible oxidation at $E_{1/2} = 0.98$ V, forming the $[Re_2(\mu\text{-}S)_2(S_2COCH_2CH(CH_3)_2)_4]^{2+}$ complex (Re^{V}, Re^{V}). Beyond −1.60 V, decomposition occurs. The reduction at 0.98 V is not observed when excess sulfur is present in the product (Figure 6b). In addition, a new broad reduction peak is observed at −0.10 V and the reversible systems become quasi-reversible in the presence of excess sulfur.

(22) (a) Snow, M. R.; Tiekink, E. R. T.; Young, C. G. *Inorg. Chim. Acta* **1988**, *150*, 161−162. (b) Young, C. G.; Kocaba, T. O.; Sadek, M.; Brownlee, R. T. C.; Tiekink, E. R. T. *Aust. J. Chem.* **1994**, *47*, 2075−2085.

(23) Fedin, V. P.; Mironov, Yu. V.; Virovets, A. V.; Podberezskaya, N. V.; Fedorov, V. Ye.; Semyannikov, P. P. *Polyhedron* **1992**, *11*, 279−284.

(24) (a) Dirand, J.; Ricard, L.; Weiss, R. *Inorg. Nucl. Chem. Lett.* **1975**, *11*, 661−664. (b) Dirand-Colin, J.; Schappacher, M.; Ricard, L.; Weiss, R. *J. Less-Common Met.* **1977**, *54*, 91−99. (c) Leonard, K.; Plute, K.; Haltiwanger, R. C.; Rakowski DuBois, M. *Inorg. Chem.* **1979**, *18*, 3246−3251.

(25) Young, C. G.; Broomhead, J. A.; Boreham, C. J. *J. Chem. Soc., Dalton Trans.* **1983**, 2135−2138.

(26) Dirand, J.; Ricard, L.; Weiss, R. *J. Chem. Soc., Dalton Trans.* **1976**, 278−282.

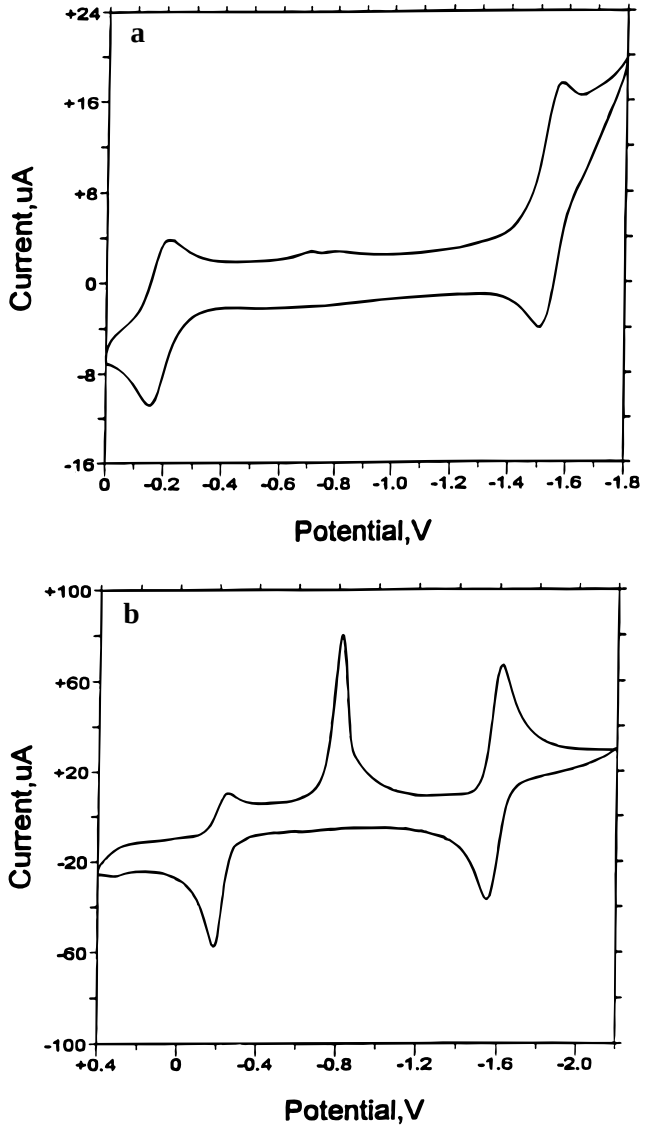

Figure 5. (a) Cyclic voltammogram of 0.01 M $[Et_4N][Re_2(\mu\text{-}S)_2(\mu\text{-}S_2)(\mu\text{-}S_2COCH_2CH(CH_3)_2)(S_2COCH_2CH(CH_3)_2)_2]$, with 0.1 M Bu_4NPF_6 in CH_3CN vs $Ag/AgNO_3$. (b) Cyclic voltammogram of an older sample of $[Et_4N][Re_2(\mu\text{-}S)_2(\mu\text{-}S_2)(\mu\text{-}S_2COCH_2CH(CH_3)_2)(S_2COCH_2CH(CH_3)_2)_2]$, which has undergone some decomposition (run under the same conditions as in (a) above).

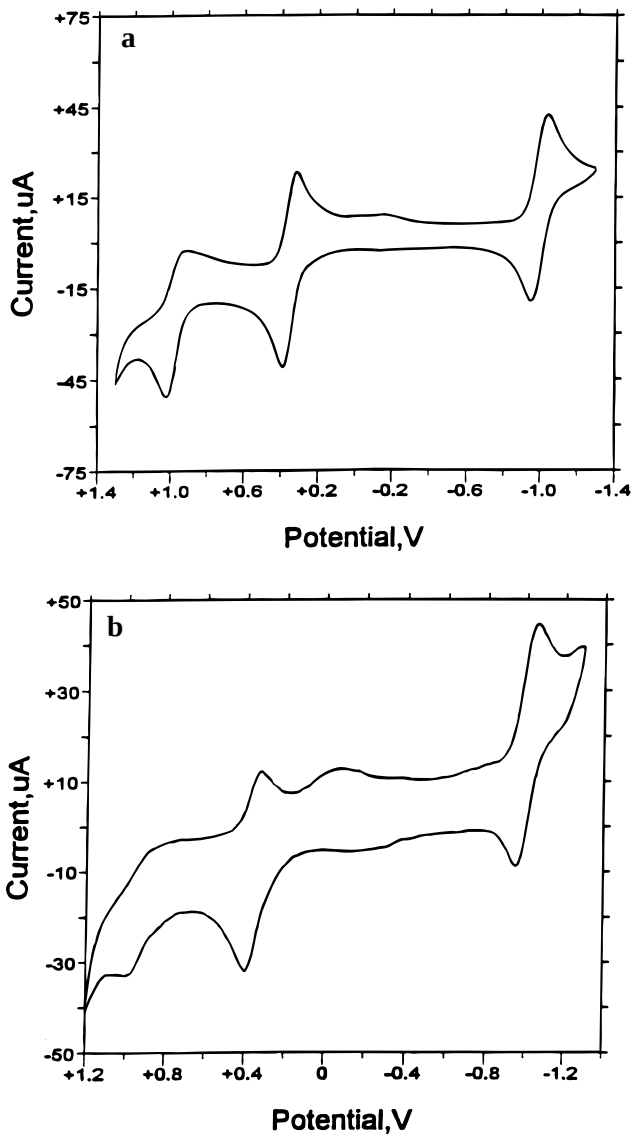

Figure 6. (a) Cyclic voltammogram of a pure sample of 0.01 M $[Re_2(\mu\text{-}S)_2(S_2CO\ CH_2CH(CH_3)_2)_4]$, with 0.1 M Bu_4NPF_6 in CH_2Cl_2 vs $Ag/AgNO_3$. (b) Cyclic voltammogram of a sample of $[Re_2(\mu\text{-}S)_2(S_2COCH_2\text{-}CH(CH_3)_2)_4]$ containing a sulfur impurity (run under the same conditions as in (a) above).

The cyclic voltammogram of $[Re(S_2CC_6H_5)(S_3CC_6H_5)_2]$ in CH_2Cl_2 (vs $Ag/AgNO_3$) is shown in Figure 7. Two reversible, one-electron oxidations (580 and 994.5 mV) are observed. Cathodic scans reveal one irreversible reduction at −1.09 V. Scanning below −1.5 V results in decomposition of the complex. The two reversible oxidations are assigned to the formation of Re(IV) and Re(V), respectively, presumably accessing the $5d^3$ [Re(IV)] and $5d^2$ [Re(V)] systems.

Discussion

Ligand Effects. The reaction between $[Et_4N][ReS_4]$ and dialkylxanthogen disulfide $[(ROCS_2)_2]$ is typical of induced internal electron transfer reactions. In this reaction, Re^{VII} undergoes a three-electron reduction to Re^{IV}, producing the red, anionic dinuclear complex $[Re^{IV}_2(\mu\text{-}S)_2(\mu\text{-}S_2)(S_2COR)_3]^-$:

$$2[Re^{VII}S_4]^- + 2[ROCS_2]_2 \rightarrow [Re^{IV}_2(\mu\text{-}S)_2(\mu\text{-}S_2)(S_2COR)_3]^- + 4\text{“}S^0\text{”} + [ROCS_2]^- \quad (2)$$

The electrons come from the oxidation of S^{2-} with the following electron count showing the redox balance:

$$2Re^{VII} + 2(3e^-) \rightarrow 2Re^{IV} \qquad (6\text{-}e^- \text{ redn})$$

$$6S^{2-} \rightarrow S_2^{2-} + 4\text{“}S^0\text{”} + 10e^- \qquad (10\text{-}e^- \text{ oxidn})$$

$$2(ROCS_2)_2 + 4e^- \rightarrow 3(ROCS_2)^- + (Et_4N)(ROCS_2) \qquad (4\text{-}e^- \text{ redn})$$

In the similar reaction between $[ReS_4]^-$ and tetraalkylthiuram disulfide, (1), Re^{VII} undergoes a three-electron reduction to Re^{IV}, forming the green, neutral dimer $[Re_2(\mu\text{-}S)_2(S_2CNR_2)_4]$. In contrast, Re^{VII} undergoes an unprecedented four-electron reduction to Re^{III} in the reaction of dithiobenzoate disulfide with $[ReS_4]^-$, producing the green, neutral mononuclear complex $[Re^{III}(S_2CC_6H_5)(S_3CC_6H_5)_2]$:

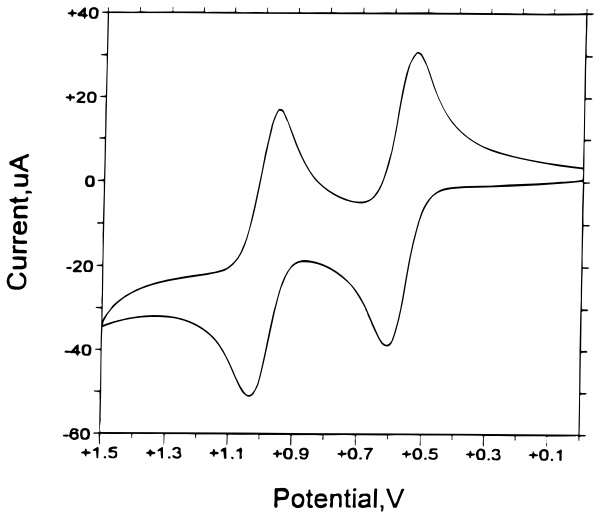

Figure 7. Cyclic voltammogram of $[Re(S_2CC_6H_5)(S_3CC_6H_5)_2]$: 0.01 M complex, 0.1 M Bu_4NPF_6 in CH_2Cl_2, 0−1.5 V, 100 mV/s, $Ag/AgNO_3$ reference electrode.

$$[Et_4N]Re^{VII}S_4 + 2(C_6H_5CS_2)_2 \rightarrow [Re^{III}(S_2CC_6H_5)(S_3CC_6H_5)_2] + 2\text{“}S^0\text{”} + [Et_4N]S_2CC_6H_5 \quad (3)$$

The balanced electron count is

$$Re^{VII} + 4e^- \rightarrow Re^{III} \quad (4\text{-}e^- \text{ redn})$$

$$2(C_6H_5CS_2)_2 + 4e^- \rightarrow 4(C_6H_5CS_2)^- \quad (4\text{-}e^- \text{ redn})$$

$$4S^{2-} \rightarrow 4\text{“}S^0\text{”} + 8e^- \quad (8\text{-}e^- \text{ oxidn})$$

In all of the above equations, “S^0” represents free sulfur (identified by UV−vis/NIR and IR spectra as a reaction byproduct). In the dithiobenzoate disulfide reaction, “S^0” also includes one of the sulfur atoms in the perthio bond of each $(S_3CC_6H_5)^-$ ligand.

Important differences in reactions 1−3 involve the degree of rhenium reduction and the type of product formed. Rhenium undergoes a three-electron reduction in reactions 1 and 2 but undergoes a four-electron reduction in reaction 3. Reaction 1 yields an anionic dimer, reaction 2 forms a neutral dimer, and reaction 3 forms a neutral monomer. What factors influence the formation of these three different products from closely related reactions?

During the reaction between $[ReS_4]^-$ and $[(ROCS_2)_2]$ (in which $Re^{IV}_2(\mu\text{-}S)_2(\mu\text{-}S_2)(\mu\text{-}S_2COR)(S_2COR)_2^-$ is the major product), a small amount of green $[Re_2(\mu\text{-}S)_2(S_2COR)_4]$, **2**, is obtained. Complex **2**, identified by comparison of IR and UV−vis spectra with those of the known compound $[Re_2(\mu\text{-}S)_2(S_2CNR_2)_4]$,[4a] could not be isolated in measurable yield from the induced internal electron transfer between $[ReS_4]^-$ and dialkylxanthogen disulfide (even in the presence of excess disulfide). However, **2** could be isolated in a modest yield (31%) via a redox reaction between $ReCl_5$ and the xanthate salt $K[S_2COR]$ (where R = *n*-butyl or isobutyl). UV−vis spectra of a red byproduct isolated from the reaction showed that diisobutyl xanthogen disulfide was formed, indicating that potassium isobutylxanthate was the reducing agent.

Why is $[Re_2(\mu\text{-}S)_2(\mu\text{-}S_2)(\mu\text{-}S_2COR)(S_2COR)_2]^-$ formed instead of $[Re_2(\mu\text{-}S)_2(S_2COR)_4]$ during the induced internal electron transfer reaction between $[ReS_4]^-$ and $[(ROCS_2)_2]$? Before addressing this question, we discuss the outcome of two other reactions involving diethylxanthogen disulfide, $[(CH_3CH_2OCS_2)_2]$ and diisobutylthioxanthogen disulfide, $[(S_2CSCH_2CH(CH_3)_2)_2]$, with $[ReS_4]^-$.

Ligand Decomposition. The reaction of $[(CH_3CH_2OCS_2)_2]$ with $[Et_4N][ReS_4]$, carried out under the same conditions as those for the reaction of $[((CH_3)_2CHCH_2OCS_2)_2]$ with $[Et_4N][ReS_4]$, did not proceed to completion. Addition of excess diethylxanthogen disulfide had no effect on product yield. IR and UV−vis spectra revealed mainly unreacted $[Et_4N][ReS_4]$ and xanthogen disulfide. This difference in reactivity can be attributed to two factors: (1) the decomposition rates of xanthogen disulfides and (2) the difference in redox potentials between diethyl-, diisopropyl-, and diisobutylxanthogen disulfides.

Xanthate ions and dixanthogens are prone to decomposition, even under mild conditions.[11] Depending on the solvent, xanthate ions either (1) decompose to carbon disulfide and the corresponding alcohol, (2) hydrolyze to form the monothiocarbonate ion $[ROC(O)S]^-$, or (3) form “sulfur xanthates” (shown following), with the decomposition rates varying in the order

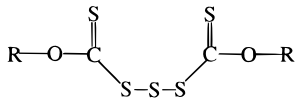

methyl ≫ ethyl > propyl > butyl.[11] This decomposition is evident in the cyclic voltammogram of $[(CH_3CH_2)_4N][Re_2(\mu\text{-}S)_2(\mu\text{-}S_2)(\mu\text{-}S_2COR)(S_2COR)_2]$, where an irreversible reduction peak is observed at −0.77 V (vs $Ag/AgNO_3$, Figure 5b). This reduction peak could be due to either monothiocarbonate or “sulfur xanthate”, as both are electrochemically active, with reduction potentials in the appropriate potential range (around −0.77 V).[11]

The redox potential of xanthogens becomes progressively more negative with increasing chain length.[11a,b] Hence, the shortest alkyl chain xanthogens are the easiest to reduce and the fastest to decompose. The reported $E°$ (vs NHE) values for ethyl, isopropyl, and *n*-butyl xanthate are −0.057, −0.089, and −0.128 V, respectively.[11b] The difference between these potentials may be large enough to affect the reaction rate, causing the reaction with diethylxanthogen disulfide to be incomplete compared to the analogous reactions with diisopropyl- and diisobutylxanthogen disulfides. In addition to ligand decomposition, decomposition of the rhenium xanthate complexes also occurs. For example, **1** decomposes slowly (several months) as a solid under an inert atmosphere and more quickly (several days) in solution.

Interestingly, mixing a 4:1 ratio of $[((CH_3)_2CHCH_2SCS_2)_2]$ to $[Et_4N][ReS_4]$ under the same conditions as for the reaction of $[((CH_3)_2CHCH_2OCS_2)_2]$ with $[Et_4N][ReS_4]$ did not yield any reaction. Even after stirring the reactants for over a week and then refluxing in CH_3CN, we observed no change in the UV−vis spectra. This lack of reactivity could be due to decomposition of thioxanthogens,[27] or to the redox potential of the disulfide, as will be discussed below.

Ligand Redox Trends. The relative ease of reduction of complexes follows the orders (decreasing left to right) thioxanthate $[(S_2CSR)^-]$ > xanthate $[(S_2COR)^-]$ > dithiophosphate $[(S_2P(OR)_2)^-]$ > dithiocarbamate $[(S_2CNR_2)^-]$, for $Mo_4S_4L_6$ cubanes, and dithiobenzoate > thioxanthate > xanthate > dithiocarbamate, for Mo_2L_4 dimers.[12,28] These same trends apply to $[Re_2(\mu\text{-}S)_2(S_2COCH_2CH(CH_3)_2)_4]$ and the analogous dithio-

(27) Coucouvanis, D.; Lippard, S. J.; Zubieta, J. A. *J. Am. Chem. Soc.* **1970**, *92*, 3342−3347.

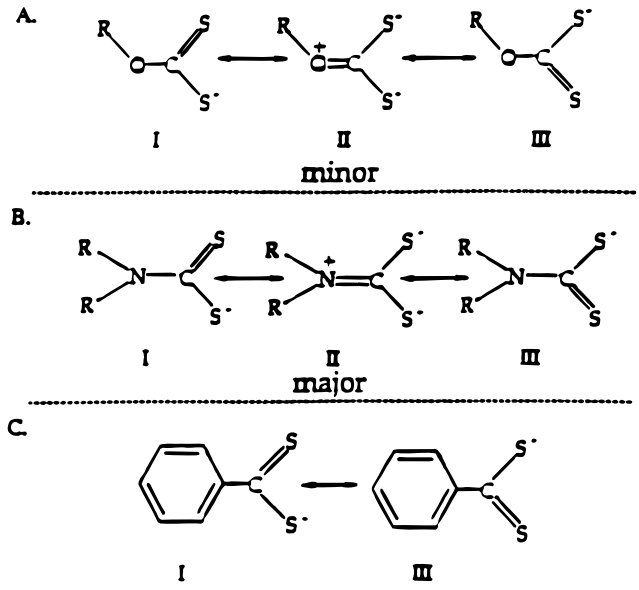

Figure 8. Resonance structures of xanthate (A), dithiocarbamate (B), and dithiobenzoate (C).

carbamate complex $[Re_2(\mu\text{-}S)_2(S_2CN(CH_3)_2)_4]$. Comparing the cyclic voltammograms of $[Re_2(\mu\text{-}S)_2(S_2CN(CH_3)_2)_4]$ and $[Re_2(\mu\text{-}S)_2(S_2COCH_2CH(CH_3)_2)_4]$, we see that the xanthate complex is easier to reduce (1.35, 0.72, −0.63 V vs SCE) than the dithiocarbamate complex (0.76, 0.17, −1.15 V vs SCE).[4a]

The ease of reduction of the complex is related to the ease of reduction of the ligand, which, in turn, is related to the electron-releasing or electron-withdrawing effects of the ligand substituent.[12] These effects can be attributed to particular resonance structures that dominate in a given ligand (Figure 8).[19] For dithiobenzoate, structures **I** and **III** are the only significant resonance forms. Structure **II** is expected to contribute more strongly in the dithiocarbamate than in the xanthate or thioxanthate systems,[19] consistent with dithiocarbamate as the best electron donor. In summary, the placement of negative charge on the sulfur atoms enhances the electron-donating characteristics of ligands, which increase in the order $(C_6H_5CS_2)^-$ < $(RSCS_2)^-$ < $(ROCS_2)^-$ < $(R_2NCS_2)^-$.[12,19,29] Hence, dithiocarbamate should be able to stabilize a higher oxidation state than either xanthate, thioxanthate, or dithiobenzoate.

The difference in electron-donating ability correlates with the observed reactivity trend of dithiocarbamate, xanthate, thioxanthate, and dithiobenzoate with $[Et_4N][ReS_4]$. The dithiobenzoate ligand, the weakest electron donor, forms the lowest oxidation state (Re^{III}), while both the dithiocarbamate and xanthate ligands form Re^{IV} complexes (see Table 5). Between dithiocarbamate and xanthate, the better electron-withdrawing ligand (xanthate) is associated with an anionic complex. If the reaction of tetraalkylthiuram disulfide with $[ReS_4]^-$ is carried out in a 1:1 CH_3CN/CH_2Cl_2 solution, a cationic complex, $[Re(S_2CNR_2)_4][Cl]$, is isolated.[4a] The better electron-donating ligand (dithiocarbamate) can clearly stabilize the greater positive charge in the Re(V) complex. This effect is likely an important factor in the isolation of a disulfide-bridged xanthogen complex, $[Re_2(\mu\text{-}S)_2(\mu\text{-}S_2)(\mu\text{-}S_2COR)(S_2COR)_2]^-$, compared to the dithiocarbamate complex $[Re_2(\mu\text{-}S)_2(S_2CNR_2)_4]$. The negatively charged disulfide complex is probably destabilized when dithiocarbamate ligands are present due to their electron-donating nature.

Table 5. Summary of Internal Electron Transfer Reactions between Tetrathiometalates and 1,1-Dithiolate Disulfides

MS_4^{n-}	1,1-dithiolate disulfide	product	ref
$W^{VI}S_4^{2-}$	$(S_2CNR_2)_2$	$W^{VI}S(S_2)(S_2CNR_2)_2$	4c
$Mo^{VI}S_4^{2-}$	$(S_2CNR_2)_2$	$Mo^{V}S_2(S_2CNR_2)_3$	4c
$Re^{VII}S_4^-$	$(S_2CNR_2)_2$	$Re^{IV}{}_2(\mu\text{-}S)_2(S_2CNR_2)_4$	4a,d
$Mo^{VI}S_4^{2-}$	$(C_6H_5CS_2)_2$	$Mo^{IV}(S_2CC_6H_5)_4$	this paper 13,14
$Re^{VII}S_4^-$	$(C_6H_5CS_2)_2$	$Re^{III}(S_2CC_6H_5)(S_3CC_6H_5)_2$	this paper
$Re^{VII}S_4^-$	$(ROCS_2)_2$	$[Re^{IV}{}_2(\mu\text{-}S)_2(\mu\text{-}S_2)(S_2COR)_3]^-$	this paper
$W^{VI}S_4^{2-}$	S_8	$[W^{V}{}_2S_2(\mu\text{-}S)_2(S_4)_2]^{2-}$	15
$Mo^{VI}S_4^{2-}$	S_8	$[Mo^{IV}S(S_4)_2]^{2-}$	4e
$Re^{VII}S_4^-$	S_8	no reaction	this paper

Tetrathiometalate Effects. Another major determinant of the reaction course is the redox strength of the tetrathiometalate. Comparison of the reaction of dithiobenzoate disulfide with $[Re^{VII}S_4]^-$, $[Mo^{VI}S_4]^{2-}$, and $[W^{VI}S_4]^{2-}$ shows that rhenium undergoes a four-electron reduction, to form $[Re^{III}(S_2CC_6H_5)(S_3CC_6H_5)_2]$, molybdenum undergoes a two-electron reduction, to form $[Mo^{IV}(S_2CC_6H_5)_4]$, and tungsten undergoes no reduction at all, forming $[W^{VI}S(S_2)(S_2CC_6H_5)_2]$ by pure ligand redox (see Table 5). With tetraalkylthiuram disulfide, the same trend holds (though details differ) with rhenium undergoing a three-electron reduction, to form $[Re^{IV}{}_2(\mu\text{-}S)_2(S_2CNR_2)_4]$,[4a,d] molybdenum undergoing a one-electron reduction, to form $[Mo^{V}S_2(S_2CNR_2)_3]$,[4c] and tungsten again undergoing no reduction, forming $[W^{VI}S(S_2)(S_2CNR_2)_2]$ (Table 5).[4c]

Why does rhenium undergo the largest reduction, while tungsten undergoes no reduction at all? Ligand-to-metal charge transfer (LMCT) energy bands of tetrathiometalates present a possible parameter for correlating the extent of metal reduction in induced internal redox reactions. The position of the lowest energy LMCT band ($LMCT_1$) reflects the energy it takes to move an electron from the sulfide to the metal center of a tetrathiometalate anion. Looking at $LMCT_1$ band energies, one sees that $[W^{VI}S_4]^{2-}$ has the highest $LMCT_1$ band at 25.5×10^3 cm^{-1}, $[Mo^{VI}S_4]^{2-}$ is next with $LMCT_1 = 21.4 \times 10^3$ cm^{-1}, and $[Re^{VII}S_4]^-$ has the lowest $LMCT_1$ band at 19.8×10^3 cm^{-1}.[30] As a result, it takes less energy to move an electron from S to Re than from S to W, and reaction of the three tetrathiometalates with either dithiobenzoate disulfide or tetraalkylthiuram disulfide, leads to rhenium undergoing the largest reduction, followed by molybdenum and then tungsten, which is not reduced at all. "Inactivity" toward metal reduction in $[W^{VI}S_4]^{2-}$ is consistent with the relatively high $LMCT_1$ energy band, making the pathway for internal electron transfer energetically unfavorable. Thus, the reaction occurs by the energetically more favorable ligand redox pathway. In comparison, the $LMCT_1$ of $[W^{VI}Se_4]^{2-}$, 21.6×10^3 cm^{-1}, is similar to that of $[Mo^{VI}S_4]^{2-}$.[30] The reaction of $[W^{VI}Se_4]^{2-}$ with $(R_2NCS_2)_2$ is analogous to the reaction of $[Mo^{VI}S_4]^{2-}$ with $(R_2NCS_2)_2$. Both follow an internal electron transfer pathway to produce $W^{V}Se_2(R_2NCS_2)_3$ and $Mo^{V}S_2(R_2NCS_2)_3$, respectively.[31] Thus, the $LMCT_1$ energy band of the tetrathiometalate is potentially predictive of the oxidation state level achieved in the final product.

The trends discussed above are generally useful but are not invariably followed. For example, $[W^{VI}S_4]^{2-}$ only reacts with

(28) Coyle, C. L.; Eriksen, K. A.; Farina, S.; Francis, J.; Gea, Y.; Greaney, M. A.; Guzi, P. J.; Halbert, T. R.; Murray, H. H.; Stiefel, E. I. *Inorg. Chim. Acta* **1992**, *198*−*200*, 565−575.
(29) Mattson, B. M.; Heiman, J. R.; Pignolet, L. H. *Inorg. Chem.* **1976**, *15*, 564−571.
(30) Müller, A.; Diemann, E.; Jostes, R.; Bögge, H. *Angew. Chem., Int. Ed. Engl.* **1981**, *20*, 934−955.
(31) Gea, Y.; Greaney, M. A.; Coyle, C. L.; Stiefel, E. I. *J. Chem. Soc., Chem. Commun.* **1992**, 160−161.

S_8 upon heating, to form $[W^{V}_2S_2(\mu\text{-}S)_2(S_4)_2]^{2-}$, and $[Mo^{VI}S_4]^{2-}$ reacts with S_8 at room temperature, to produce $[Mo^{IV}S(S_4)_2]^{2-}$ (Table 5).[4b,4e,18] However, $[Re^{VII}S_4]^-$ does not react at all with S_8 (Table 5). Since the reactant is the same, one may expect the LMCT energies of the tetrathiometalates to influence the course of the reactions. Though the reactions of $[W^{VI}S_4]^{2-}$ and $[Mo^{VI}S_4]^{2-}$ with sulfur seem to follow LMCT trends, the reaction of $[Re^{VII}S_4]^-$ (with the lowest $LMCT_1$ energy band) with sulfur deviates from this pattern. In addition, $[Mo^{VI}S_4]^{2-}$ reacts with diphenyl disulfide, $C_6H_5SSC_6H_5$, to produce $[Mo_2S_8]^{2-}$,[32] but $[Re^{VII}S_4]^-$ does not react (even at elevated temperatures) with $C_6H_5SSC_6H_5$. Though these reactions do not deal with 1,1-dithiolate disulfides, they do involve (or potentially involve) induced internal electron transfers and, as such, are probably influenced by some of the same factors discussed above for the 1,1-dithiolate disulfide reactions.

In both cases mentioned above (reaction with sulfur and reaction with diphenyl disulfide), the $[ReS_4]^-$ anion deviates from the trends. Müller et al. noted that the LUMO of $[ReS_4]^-$ contains more S contributions, compared to the LUMO of $[MoS_4]^{2-}$, which corresponds to a stronger Re−S interaction.[33] Along the same lines, Hartree−Fock−Slater orbital energies show that the Re-5d and S-3p orbital energies are very similar (S-3p, 10.3; Mo-4d, 7.2; W-5d, 9.3; Re-5d, 10.6 eV),[34] and thus, ligand and metal orbitals mix better in Re−S compounds than in analogous Mo and W compounds. In addition, there is a shorter M−S bond in $[ReS_4]^-$ (2.155 Å) than in $[MoS_4]^{2-}$ and $[WS_4]^{2-}$ (2.178 and 2.177 Å, respectively).[33] Perhaps these differences in rhenium−sulfur orbital interactions and bond strength have a dominating influence on kinetics of $[ReS_4]^-$ reactions under certain conditions.

Conclusions

Reaction of $[Et_4N][Re^{VII}S_4]$ with dialkylxanthogen disulfide results in an internal redox reaction that produces the anionic complex $[Re^{IV}_2(\mu\text{-}S)_2(\mu\text{-}S_2)(S_2COR)_3]^-$. In contrast, $[Re^{IV}_2(\mu\text{-}S)_2(S_2CNR_2)_4]$ and $[Re^{III}(S_2CC_6H_5)(S_3CC_6H_5)_2]$ are the major products obtained from the reaction of $[Et_4N][Re^{VII}S_4]$ with tetraalkylthiuram disulfide and dithiobenzoate disulfide, respectively. The diverse results are attributable to differences in electron-donating abilities of the corresponding ligands, where dithiocarbamate is the strongest electron donor and dithiobenzoate the weakest. The xanthate analogue of the dithiocarbamate complex can only been obtained (in a reasonable yield) by the redox reaction between $ReCl_5$ and the xanthate salt $K[S_2COR]$. Comparing the electrochemistry of the neutral xanthate dinuclear complex $[Re_2(\mu\text{-}S)_2(S_2COCH_2CH(CH_3)_2)_4]$ with that of the neutral dithiocarbamate dinuclear complex $[Re_2(\mu\text{-}S)_2(S_2CN(CH_3)_2)_4]$ confirms that trends previously established are followed in the metal sulfide systems discussed in this paper (i.e., dithiocarbamate complexes are harder to reduce than xanthate complexes due to the better electron-donating ability of the dithiocarbamate ligand).

Holding the ligand constant while varying the tetrathiometalate gives a set of reactions where the nature of the products correlates with the ligand-to-metal charge transfer energy (LMCT). Thus $[W^{VI}S_4]^{2-}$, with the highest $LMCT_1$ (25.3×10^3 cm^{-1}),[30] was not reduced when reacted with either dithiobenzoate disulfide or tetraalkylthiuram disulfide. Apparently, the high $LMCT_1$ energy band disfavors an internal electron transfer path in which tungsten is reduced. Instead, ligand redox occurs (Table 5). In comparison, $[Re^{VII}S_4]^-$ ($LMCT_1 = 19.8 \times 10^3$ cm^{-1})[30] undergoes the largest reduction (four-electron reduction with dithiobenzoate disulfide, three-electron reduction with thiuram disulfide), while $[Mo^{VI}S_4]^{2-}$ ($LMCT_1 = 21.3 \times 10^3$ cm^{-1}) falls between (two- and one-electron reductions for dithiobenzoate and thiuram disulfides, respectively).

Reactions involving $[W^{VI}S_4]^{2-}$, $[Mo^{VI}S_4]^{2-}$, and $[Re^{VII}S_4]^-$ with S_8 and diphenyl disulfide seemingly deviate from the trends discussed above. Here reactions involving both $[W^{VI}S_4]^{2-}$ and $[Mo^{VI}S_4]^{2-}$ follow LMCT energies (forming $[W^{V}_2S_2(\mu\text{-}S)_2(S_4)_2]^{2-}$ and $[Mo^{IV}S(S_4)_2]^{2-}$, respectively) but no reaction (though carried out under various conditions and stoichiometries) occurs with $[Re^{VII}S_4]^-$, thus departing from LMCT reactivity trends. Clearly, induced internal electron transfer reactions are influenced by factors other than the donor/acceptor ability of the ligand and the ligand-to-metal charge transfer energy of the tetrathiometalate. Continued research to broaden the scope of induced internal electron transfer reactions will be important in helping to understand these overall trends.

Supporting Information Available: Listings of crystal data, structure refinement details, atomic coordinates, thermal parameters, bond lengths, and bond angles for **1**, **2**, and **5**. This material is available free of charge on the Internet at http://pubs.acs.org.

IC980674Z

(32) Coyle, C. L.; Harmer, M. A.; George, G. N.; Daage, M.; Stiefel, E. I. *Inorg. Chem.* **1990**, *29*, 14−19.
(33) Müller, A.; Krickemeyer, E.; Wittneben, V.; Bögge, H.; Lemke, M. *Angew. Chem., Int. Ed. Engl.* **1991**, *30*, 1512−1514.
(34) Yeh, J. J.; Lindau, I. *At. Data Nucl. Data Tables* **1985**, *32*, 1.